

# Deep Metric Learning with Alternating Projections onto Feasible Sets

Oğul Can\* Yeti Z. Gürbüz† A. Aydın Alatan‡

Dept. of Elect. and Elec. Eng. & Center for Image Analysis (OGAM)

Middle East Technical University

Ankara, Turkey, 06800

\*ogul.can@metu.edu.tr, †ygurbuz@metu.edu.tr, ‡alatan@metu.edu.tr

## Abstract

During the training of networks for distance metric learning, minimizers of the typical loss functions can be considered as "feasible points" satisfying a set of constraints imposed by the training data. To this end, we reformulate deep metric learning problem as finding a feasible point of a constraint set where the embedding vectors of the training data satisfy desired intra-class and inter-class proximity. The feasible set induced by the constraint set is expressed as the intersection of the relaxed feasible sets which enforce the proximity constraints only for particular samples (a sample from each class) of the training data. Then, the feasible point problem is to be approximately solved by performing alternating projections onto those feasible sets. Such an approach results in minimizing a typical loss function with a systematic batch set construction where these batches are constrained to contain the same sample from each class for a certain number of iterations. Moreover, these particular samples can be considered as the class representatives, allowing efficient utilization of hard class mining during batch construction. The proposed technique is applied with the contrastive, triplet, lifted structured,  $N$ -pair, angular and margin-based losses and evaluated on Stanford Online Products, CAR196 and CUB200-2011 datasets for image retrieval and clustering. The proposed approach outperforms state-of-the-art for all 6 loss functions with no additional computational cost and boosts its performance further by hard negative class mining.

## 1 Introduction

Distance metric learning (DML) is the problem of finding a proper function that satisfies metric axioms and assesses the semantic dissimilarity of the data samples from its domain. This task is generally realized by learning proper representations for the data samples so that the semantically similar ones are embedded to the small vicinity in the representation space as the dissimilar samples are placed relatively apart in the Euclidean sense. The representations are learned through an optimization framework in which the objective function utilizes the loss terms to impose the desired intra-class and inter-class proximity constraints in the representation space [1–10]. The optimization is performed with mini-batch gradient updates and the procedure is generally guided by providing deliberately selected exemplars [2, 3, 8, 11–13].

In this work, we revisit the proximity constraints in the representation space implied by the loss terms for proper DML. To develop a general framework for DML, we focus on finding a feasible point satisfying the proximity constraints. Our formulation results in subproblems to be solved by minimizing the regularized version of the typical loss functions for DML with a systematic batch construction where the batches are constrained to contain a particular sample from each class for a certain number of iterations. That structure allows efficient utilization of hard negative class mining (HNCM) during batch construction to guide the optimization without offline processing.

## 2 Notations and Definitions

We consider dataset of two-tuples,  $\{(x_i, y_i)_{i \in \mathcal{N}} \mid i \in \mathcal{N}\}$ , where  $x_i \in \mathcal{X}$  denotes a sample vector from the data space (e.g. images),  $y_i \in \mathcal{Y} = \{1, \dots, L\}$  denotes the corresponding label of the sample among  $L$  many classes and  $\mathcal{N} = \{1, \dots, N\}$  denotes the set of indexes to represent samples from the dataset of size  $N$ . Indicator of the two samples indexed by  $i$  and  $j$  belonging to the same class is denoted as  $y_{i,j} \in \{0, 1\}$  where  $y_{i,j} = 1$  if  $y_i = y_j$ . We call  $j$  positive/negative sample for  $i$  if  $y_{i,j} = 1/0$ .

The parametric distance between two samples  $x_i$  and  $x_j$  is defined as:

$$d_{i,j}^f(\theta) \triangleq \|f(x_i; \theta) - f(x_j; \theta)\|_2 \quad (2.1)$$

which is the Euclidean distance equipped with a  $D$ -dimensional vector valued parametric function,  $f : \mathcal{X} \xrightarrow{f} \mathbb{R}^D$ , with parameters  $\theta$ . The projection of  $\theta$  onto a set  $\mathcal{S}$  is defined as:

$$\mathcal{P}_{\mathcal{S}}(\theta) \triangleq \arg \min_{\vartheta \in \mathcal{S}} \frac{1}{2} \|\theta - \vartheta\|_2^2. \quad (2.2)$$

For a set defined by an inequality  $\mathcal{S} = \{\theta \mid g(\theta) \leq 0\}$ , we denote its indicator as  $\iota_{\mathcal{S}}(\theta)$  which is:

$$\iota_{\mathcal{S}}(\theta) \triangleq \lim_{\lambda \rightarrow 0} \left[ \frac{1}{\lambda} g(\theta) \right]_+, \quad (2.3)$$

where  $[z]_+ = \max\{0, z\}$  and  $g(\cdot)$  is an arbitrary function. We are to approximate  $\iota_{\mathcal{S}}(\theta)$  for small  $\lambda$  as

$$\hat{\iota}_{\mathcal{S}}(\theta) \approx \frac{1}{\lambda} [g(\theta)]_+. \quad (2.4)$$

## 3 Review of the Related Works

We restrict ourselves to the distance metric learning problem which is posed as learning the parameters,  $\theta$ , of an embedding function,  $f(\cdot; \theta)$ , so that the parametric distance,  $d_{i,j}^f(\theta)$ , between the data samples reflects their semantic dissimilarity.  $f$  as a linear mapping is considered in earlier approaches [10, 14, 15] that later inspire most of state-of-the-art frameworks [1–9] in which  $f$  is a nonlinear mapping realized by deep neural networks.

Learning a proper linear mapping for the parametric distance is initially formulated as a convex optimization problem in [14]. The objective is minimizing the parametric distances among the samples of the same classes. To prevent null mappings, a constraint that enforces mapping of the samples from different classes to be at least separated by some margin is added to the formulation. Moving that constraint to the objective via hinge loss [1] results in the well-known contrastive loss:

$$\mathcal{L}_{\text{contrastive}}(\theta; \mathcal{P}) = \frac{1}{|\mathcal{P}|} \sum_{(i,j) \in \mathcal{P}} y_{i,j} d_{i,j}^f(\theta)^2 + (1 - y_{i,j}) [\varepsilon - d_{i,j}^f(\theta)]_+^2, \quad (3.1)$$

where  $\mathcal{P}$  is the set of pairs and  $\varepsilon$  is the desired margin. Minimizing the contrastive loss embeds the samples from the same class in a neighborhood as small as possible. This approach ignores the intra-class variations of the classes and results in internally diverse classes to be treated equally as internally similar classes. Triplet loss introduced in [15] and popularized in deep metric learning frameworks [2, 12] alleviates this problem by constraining the distance to any positive sample to be at least some margin smaller than the distance to any negative sample for each sample:

$$\mathcal{L}_{\text{triplet}}(\theta; \mathcal{T}) = \frac{1}{|\mathcal{T}|} \sum_{(i,j^+,j^-) \in \mathcal{T}} [d_{i,j^+}^f(\theta)^2 - d_{i,j^-}^f(\theta)^2 + \varepsilon]_+, \quad (3.2)$$

where  $\mathcal{T}$  is the set of triplets,  $j^+$  and  $j^-$  are a positive and a negative sample for the sample  $i$ , respectively. Minimizing triplet loss entails deliberately selection of the triplets to have nonzero loss terms. Thus, either large batch size or mining for exemplars violating the triplet constraint is required [2]. Such an effort makes the computation of the triplet loss is less attractive than of the contrastive loss. Margin-based loss is introduced in [3] to provide the flexibility in the distribution of the classes in the embedding space without using triplets as the exemplars. It expresses the margin constraint of the triplet loss as separate loss terms of the distances between positive and negative sample pairs by relaxing the constraint of the contrastive loss on the positive pairs:

$$\mathcal{L}_{\text{margin}}(\theta; \mathcal{P}) = \frac{1}{|\mathcal{P}|} \sum_{(i,j) \in \mathcal{P}} y_{i,j} [d_{i,j}^f(\theta) - \varepsilon + \delta]_+ + (1 - y_{i,j}) [\varepsilon + \delta - d_{i,j}^f(\theta)]_+, \quad (3.3)$$

where  $\delta$  controls the separation margin and  $\varepsilon$  is a trainable parameter for the boundary between positive and negative pairs. The contrastive, triplet and margin-based loss terms are the simplest forms of the pairwise distance ranking based losses. In these losses, only 2 or 3 data samples contribute to the loss terms. On the other hand, all negative samples within the batch can also be integrated to a single triplet loss term in lifted structured loss [16]. It reformulates the triplet loss with the triplets formed by hard negative mining within the batch for each positive pair. Using log-sum-exp expression as the approximation of max operator in the mining operation, the lifted structured loss term for a positive pair gets the contribution of all the negative samples in the batch. In a different aspect, angular loss [4] that constraints the local geometry of the samples in the embedding space is proposed to better exploit the relation among triplets. Ranking in the quadruplets is also studied [5, 17–19] to improve the structure of the embedding space by considering relation among more samples.

The motivation of using the relations among more samples leads to softmax-classifier-based losses [8, 9] and clustering-based losses [6, 7]. Optimization of the clustering-based losses deviates from the typical nonlinear programming procedure of the deep metric learning frameworks. They involve additional sophisticated computations which might be quite expensive. Among softmax-classifier-based losses,  $N$ -pair loss [8] makes use of half of the negative samples in the batch for a positive pair. The batch for the  $N$ -pair loss is constructed by  $N$  samples from distinct classes and  $N$  corresponding positive samples. Each positive sample is used as a negative sample for the samples from other classes. This batch construction together with the  $N$ -pair loss formulation results in a sampled softmax-cross-entropy loss term for a classifier in which the embedding of the positive samples are considered as the sampled class vectors. In order to approximately increase the contribution of the negative samples for a positive pair to the global extent, proxies for classes are re-introduced in [9] after its linear metric learning counterpart [10]. Proxies can be considered as the representative vectors for the set of points in the embedding space. Thus, using proxies in the loss terms implicitly takes multiple data samples into account. Learning a proxy vector per class within the deep metric learning framework is quite similar to learning the class vectors of a softmax classifier with the sampled softmax-cross-entropy loss. The slight difference in [9] is the absence of the positive pair similarity term in the normalization of softmax computation.  $N$ -pair and proxy-based loss frameworks are closely related. Using proxies can be considered as sampling the same positive samples for each class in every batch of  $N$ -pair formulation. The resemblance of these methods against the classification frameworks supports the intuition of the methods that incorporates softmax classification into deep metric learning [20, 21].

To enhance the diversity of the semantic information embedded to the vector representations, ensemble techniques are also combined with deep metric learning framework [22–24]. The general idea is simply concatenating the vectors from multiple embedding functions whose parameters are learned by considering different local features of the samples. Hence, better embedding space can be obtained by integrating the vectors that are specialized to different aspects of the samples.

Apart from the advances in the loss terms, efficient sampling strategies to provide batch of exemplars to the learning algorithm also have a key role in the success of the deep metric learning frameworks [2, 3, 8, 11–13]. The aim of exemplar mining is to improve the speed of the convergence and the quality of the embeddings by providing informative exemplars which are tuples with non-trivial settings in general. Mining for such informative exemplars brings additional computational burden, since vast number of exemplars exist and all the samples should be mapped to the embedding space prior to mining. To avoid this computational burden, some frameworks performs mining in batches for semi-hard negative [2], hard-negative [11] and distance weighted sampling [3]. Similarly, a random subset of the dataset for semi-hard negative mining is also considered [8]. For global mining, hierarchical triplet loss framework [13] performs triplet mining through tree representation of the dataset, and smart mining method [12] exploits approximate nearest neighbor search. The main problem with these global approaches is requirement of the mapping of the entire dataset to the embedding space periodically, which prevents scalability to the large datasets. Different from the search based approaches, generation of synthetic hard negative samples through adversarial models is addressed in recent approaches [25, 26].

## 4 Proposed Approach

We revisit the early DML formulations [14, 15] which involve pairwise proximity constraints in the embedding space for the negative pairs. Yet, differently, we omit the positive pair distances to be minimized from the objective function and introduce it as a constraint for the constraint set of  $\theta$ .

Given a dataset of  $N$  samples,  $\{(x_i, y_i)\}_{i \in \mathcal{N}}$ , we consider the constraint set  $\mathcal{C} = \mathcal{C}^+ \cap \mathcal{C}^-$  for  $\theta$ :

$$\mathcal{C}^+ = \{\theta \mid d_{i,j}^f(\theta) \leq \varepsilon^+, \forall (i, j) \in \mathcal{N}^2, y_{i,j}=1\}, \quad (4.1a)$$

$$\mathcal{C}^- = \{\theta \mid d_{i,j}^f(\theta) \geq \varepsilon^-, \forall (i, j) \in \mathcal{N}^2, y_{i,j}=0\}. \quad (4.1b)$$

Once  $\varepsilon^+ < \varepsilon^-$ , the constraints  $\mathcal{C}^+$  and  $\mathcal{C}^-$  together enforce  $f(\cdot; \theta)$  to map the samples from the same class to some neighborhood such that no sample from any other class can be mapped to that neighborhood.

**Proposition 4.1.** Any  $\theta \in \mathcal{C}$  for some  $\varepsilon^+$  and  $\varepsilon^-$  is a global minimizer of the loss functions,  $\mathcal{L}_{contrastive}(\theta; \mathcal{P})$ ,  $\mathcal{L}_{triplet}(\theta; \mathcal{T})$  and  $\mathcal{L}_{margin}(\theta; \mathcal{P})$  defined in Eqs. (3.1)-(3.3), respectively.

*Proof.* The loss functions defined in Eqs. (3.1)-(3.3) satisfy  $\mathcal{L}_{(\cdot)}(\theta; \cdot) \geq 0$ ,  $\forall \theta$  and  $\min \mathcal{L}_{(\cdot)}(\theta; \cdot) = 0$ . Thus, it is enough to show that the proper selection of  $\varepsilon^+$  and  $\varepsilon^-$  yields  $\mathcal{L}_{(\cdot)}(\theta; \cdot) = 0$ ,  $\forall \theta \in \mathcal{C}$ . If  $\varepsilon^- = \varepsilon$ , any  $\theta \in \mathcal{C}$  results in  $\mathcal{L}_{contrastive}(\theta; \mathcal{P}) \rightarrow 0$  as  $\varepsilon^+ \rightarrow 0$ . For any  $\varepsilon^+$ , choosing  $\varepsilon^- = ((\varepsilon^+)^2 + \varepsilon)^{1/2}$  results in  $\mathcal{L}_{triplet}(\theta; \mathcal{T}) = 0$ ,  $\forall \theta \in \mathcal{C}$ . Similarly, choosing  $\varepsilon^+ = \varepsilon - \delta$  and  $\varepsilon^- = \varepsilon + \delta$  makes  $\mathcal{L}_{margin}(\theta; \mathcal{P}) = 0$ ,  $\forall \theta \in \mathcal{C}$ .  $\square$

Proposition 4.1 can be extended to the other pairwise distance based losses and suggests that finding a feasible point of  $\mathcal{C}$  is equivalent to solving the minimization of those loss functions. This is actually the restatement of the motivation of the existing approaches [1–9] in which the loss functions are developed to impose those constraints in the first place. Therefore, these methods can be considered as implicitly finding a feasible point of the constraint set via developing a loss function to be minimized. We address the problem differently by directly focusing on finding a feasible point and develop the loss function accordingly. To formulate our approach, we consider the relaxed set  $\mathcal{C}_k = \mathcal{C}_k^+ \cap \mathcal{C}_k^-$ :

$$\mathcal{C}_k^+ = \{\theta \mid d_{k_l,j}^f(\theta) \leq \varepsilon^+, \forall (l, j) \in \mathcal{Y}, j \in \mathcal{N}, y_{k_l,j}=1\}, \quad (4.2a)$$

$$\mathcal{C}_k^- = \{\theta \mid d_{k_l,j}^f(\theta) \geq \varepsilon^-, \forall (l, j) \in \mathcal{Y}, j \in \mathcal{N}, y_{k_l,j}=0\}, \quad (4.2b)$$

where  $k_l \in \{i \in \mathcal{N} \mid y_i = l\}$  denotes the index of a sample from class  $l$ . Note that the set  $\{k_l\}_{l=1}^L$  contains a sample index from each class. For all samples,  $\mathcal{C}_k$  enforces proximity constraints only relative to the particular class samples indexed by  $\{k_l\}_{l=1}^L$ . For each  $k$ , we consider distinct samples from each class such that  $\{k_l\}_{l=1}^L \cap \{k'_l\}_{l=1}^L = \emptyset$  for  $k' \neq k$ . Then,  $\mathcal{C}$  can be expressed as  $\mathcal{C} = \bigcap_{k=1}^K \mathcal{C}_k$ , where  $K$  is the total number of sets, which can be considered as the maximum number of samples for a class. Then, the feasible point problem can be reformulated as finding a point in the intersection of the sets. If the sets,  $\{\mathcal{C}_k\}_k$ , were closed and convex, the problem would be solvable by alternating projection methods [27, 28]. However, it is not uncommon to perform alternating projection methods to non-convex set intersection problems [29, 30]. Hence, we propose to solve the problem approximately by performing alternating projections onto the feasible sets  $\{\mathcal{C}_k\}_k$ . The problem becomes:

$$\theta^* = \lim_{k \rightarrow \infty} \left( \theta^{(k)} = \mathcal{P}_{\mathcal{C}_k}(\theta^{(k-1)}) \right), \quad (4.3)$$

where  $\mathcal{C}_{k+K} = \mathcal{C}_k$  and  $\theta^{(0)}$  is arbitrary. A problem instance corresponding to a projection becomes:

$$\theta^{(k)} = \mathcal{P}_{\mathcal{C}_k}(\theta^{(k-1)}) = \arg \min_{\theta \in \mathcal{C}_k} \frac{1}{2} \|\theta^{(k-1)} - \theta\|_2^2, \quad (4.4)$$

which can be written as an unconstrained problem in terms of the set indicator functions in (2.3) as:

$$\theta^{(k)} = \arg \min_{\theta} \frac{1}{2} \|\theta^{(k-1)} - \theta\|_2^2 + \sum_{(l,j) \mid y_{k_l,j}=1} \iota_{\mathcal{S}_{k_l,j}^+}(\theta) + \sum_{(l,j) \mid y_{k_l,j}=0} \iota_{\mathcal{S}_{k_l,j}^-}(\theta), \quad (4.5)$$

where  $\mathcal{S}_{k_l,j}^+ = \{\theta \mid d_{k_l,j}^f(\theta) \leq \varepsilon^+\}$ ,  $\mathcal{S}_{k_l,j}^- = \{\theta \mid d_{k_l,j}^f(\theta) \geq \varepsilon^-\}$  and  $(l, j) \in \mathcal{Y} \times \mathcal{N}$ . If the set indicator functions are to be approximated for small  $\lambda$  as  $\hat{\iota}_{\mathcal{S}}(\theta) \approx \frac{1}{\lambda} [g(\theta)]_+$ , as in Eq. (2.4), the problem becomes:

$$\theta^{(k)} = \arg \min_{\theta} \frac{\lambda}{2} \|\theta^{(k-1)} - \theta\|_2^2 + \sum_{k_l,j} y_{k_l,j} [d_{k_l,j}^f(\theta) - \varepsilon^+]_+ + (1 - y_{k_l,j}) [\varepsilon^- - d_{k_l,j}^f(\theta)]_+, \quad (4.6)$$

where  $(l, j) \in \mathcal{Y} \times \mathcal{N}$ . The resultant minimization problem for a projection step is very similar to the margin-based loss formulation [3] defined in Eq. (3.3) with a regularization term. The main difference

is the utilization of the particular class samples,  $\{k_l\}_{l \in \mathcal{Y}}$ , for the pairwise distance losses. In this point of view, the subproblems can be seen as learning embedding representations so that the particular class samples become the class representatives. This is similar to learning class representative vectors for a softmax classifier. Therefore, choosing the relaxed feasible sets as in Eqn. (4.2) implicitly integrates classification framework to the DML problem in our formulation.

To obtain the solution,  $\theta^*$ , defined in Eq. (4.3), one should cycle through the sets,  $\{\mathcal{C}_k\}_k$ , and perform projections until the convergence. The nature of the problem is non-convex. Therefore, exploiting diverse combinations of sets might improve the solution. We propose to perform projections by randomly selecting the class samples for the sets. This approach results in different feasible sets  $\{\mathcal{C}_k\}_k$  for each cycle so that the procedure does not stick to the specific sets. Performing a projection involves a minimization problem. In this perspective, either convergence can be monitored to pass the next projection or the projection operator can be approximated by  $M$  iterations of training. The latter approach gives the flexibility to control the fitting of the parameters to the subproblems. We therefore propose to use  $M$ -step approximations of the projection operators as  $\theta^{(k)} \approx \mathcal{P}_{\mathcal{C}_k}^{(M)}(\theta^{(k-1)})$  in our framework.

Proposed learning procedure for  $\theta$  necessitates utilization of the particular class samples for the loss computation. To provide scalability, those particular class samples can also be sampled during batch construction. In this manner, another implication of the proposed framework becomes imposing constraint on the batch construction for the minimization. If we disregard the resultant loss formulation in Eq. (4.6) and consider only batch construction method of our framework, we can formulate minimization of any pairwise distance ranking based loss function within the proposed batch construction method as:

$$\theta^{(k)} = \arg \min_{\theta} \frac{1}{2} \|\theta^{(k-1)} - \theta\|_2^2 + \mathcal{L}_{(\cdot)}(\theta; \mathcal{I}_k), \quad (4.7)$$

where  $(\cdot)$  can be any proper loss and  $\mathcal{I}_k$  is the index set of the exemplars defining  $\mathcal{C}_k$ . The proposed DML framework in its most general form is summarized in Algorithm 1. Alternating projections only introduces a constrained batch construction step to the standard optimization procedure.

**Hard negative class mining.** The nature of the proposed deep metric learning framework allows efficient HNCM batch construction. As  $\theta$  is projected onto the feasible sets, the set-specific class samples can be considered as the class representatives. Thus, using those representatives, approximate global mining can be efficiently performed. To this end, we store the embedding representations of the class representatives and update those representations as we sample the corresponding representatives for the batch construction. In this way, we can perform online HNCM with  $\mathcal{O}(L)$  complexity.

**Relation to linear metric learning with convex optimization.** Convex optimization formulation of linear metric learning in [14] involves similar alternating projections onto feasible sets to perform projected gradient ascent. That approach only considers the constraint set induced by the positive pairs, whereas we consider both negative and positive pair distances jointly in the feasible set.

**Relation to  $N$ -pair and proxy-based losses.** Minimization of  $N$ -pair loss [8] can be considered as performing our method by using  $M=1$  step approximation of the projection operator. Similarly, the minimization of proxy-based losses [9, 10] can be considered as a single projection operation. Therefore,  $N$ -pair and proxy-based loss formulations are to be the two extreme cases of our framework.

---

**Algorithm 1** Projection onto Feasible Sets Deep Metric Learning (PROFS)

---

```

randomly initialize parameters  $\theta^{(0)}$ , set learning rate  $\alpha$ ,  $k=0$ 
repeat
  sample  $\mathcal{R}=\{k_l \mid y_{k_l}=l\}_{l=1}^L \sim \mathcal{N}$  an example for each class // i.e., class representatives
  repeat  $M$  times //  $\theta^{(k+1)} \approx \mathcal{P}_{\mathcal{C}_k}^{(M)}(\theta^{(k)})$ 
    sample  $\mathcal{R}'=\{i_r\}_r \sim \mathcal{R}$  a subset of the class representatives // possibly via hard class mining
    sample  $\mathcal{E}=\{j_n\}_n \sim \mathcal{N}$  a batch of examples
    construct exemplar batch  $\mathcal{B}$  from  $\mathcal{R}'$  and  $\mathcal{E}$  // e.g. pairs  $(i_r, j_n)$ 
     $\theta \leftarrow \theta - \alpha \nabla_{\theta} (\frac{1}{2} \|\theta^{(k)} - \theta\|_2^2 + \mathcal{L}_{(\cdot)}(\theta; \mathcal{B}))$  // compute  $(\cdot)$  loss for batch  $\mathcal{B}$ 
   $k \leftarrow k+1$ ,  $\theta^{(k)} \leftarrow \theta$ 
until convergence

```

---

## 5 Experimental Work

We examine the effectiveness of the proposed DML framework through evaluation on the three widely-used benchmark datasets for the image retrieval and clustering tasks. We perform ablation study on the effect of  $M$ -step approximation of the projection operation as well. Throughout the section, we use PROFS to refer our framework.

### 5.1 Benchmark Datasets and Evaluation Metrics

We obtain results by utilizing three public benchmark datasets. The conventional protocol of splitting training and testing sets for a zero-shot setting [16] is followed for all datasets. Hence, no image is in the intersection of the training and the test sets. Stanford Online Products [16] dataset has 22,634 classes with 120,053 product images. The first 11,318 classes (59,551 images) are split for training and the other 11,316 (60,502 images) classes are used for testing. Cars196 [31] dataset contains 196 classes of cars with 16,185 images. The first 98 classes (8,054 images) are used for training and remaining 98 classes (8,131 images) are reserved for testing. CUB-200-2011 [32] dataset consists of 200 species of birds with 11,788 images. The first 100 species (5,864 images) are split for training, the rest of 100 species (5,924 images) are used for testing.

We follow the standard metric learning experimental protocol defined in [16] to evaluate the performance of the deep metric learning approaches for the retrieval and clustering tasks. We utilize normalized mutual information (NMI) and  $F_1$  score to measure the quality of the clustering task which is performed by conventional  $k$ -means clustering algorithm. In order to evaluate clustering performance, normalized mutual information (NMI) and  $F_1$  score are utilized. NMI computes the label agreement between predicted and groundtruth clustering assignments neglecting the permutations while  $F_1$  measures harmonic mean of the precision and recall. Furthermore, we exploit binary Recall@K metric to evaluate the performance of the retrieval task. Recall@K for a test query is 1 if at least one sample from the same class of the query is in the  $K$  nearest neighborhood of the query. The average of the Recall@K for the test queries gives the Recall@K performance on the dataset. We refer [16] for the detailed information related to these evaluation metrics.

### 5.2 Training Setup

We use Tensorflow [33] deep learning library throughout the experiments. After the images are normalized and scaled to  $256 \times 256$ , we perform  $224 \times 224$  random crop and data augmentation by horizontal mirroring as pre-processing. For the embedding function,  $f(\cdot; \theta)$ , we utilize GoogLeNet (Inception v1) [34] architecture until the output of the global average pooling layer with the parameters pretrained on ImageNet ILSVRC dataset [35]. After the pooling layer, we add a linear transformation layer (fully connected layer) to obtain the representation vectors of size 512. We fix the embedding size of the samples at 512 throughout experiments, since it is shown in [16] that the embedding size does not have a key role on comparing performances of the deep metric learning loss functions. The parameters of the linear transformation layer is randomly initialized and are learned by using 10 times larger learning rate than the pretrained parameters for the sake of fast convergence. For the hyper-parameters, our framework introduces 2 additional parameters:  $\lambda$  for regularization and  $M$  to approximate projection operation. We set the regularization term as the result of the projection based formulation,  $\lambda$ , to a small reasonable number,  $10^{-3}$ . The number of projections steps,  $M$ , is determined according to the findings of the ablation study which is presented in subsection 5.4. For the other hyper-parameters coming from adaptation of the baseline framework (*e.g.* margins, number of positive samples etc.), we follow the settings in the corresponding baseline work. For the optimization procedure, we select the base learning rate as  $10^{-4}$  for Stanford Online Products dataset whereas we utilize  $10^{-5}$  learning rate to train CUB-200-2011 and Cars196, since they tend to meet over-fitting problem due to the limited dataset size. We exploit Adam [36] optimizer for mini-batch gradient descent with a mini-batch size is 128 and default moment parameters,  $\beta_1=.9$  and  $\beta_2=.99$ . Finally, since the convergence rate of each method is different, we train all the approaches for 100 epochs and post the performance at their best epoch as in [3] instead of following the conventional procedure [16] that reports performance of deep metric learning approaches after a certain number of training iterations.

### 5.3 Baseline Methods and PROFS Framework Adaptation

We apply proposed PROFS framework with and without HNCM on the contrastive [1], triplet [2], lifted structured [16],  $N$ -pair [8], angular [4] and margin-based [3] loss functions in order to directly compare with the state-of-the-art methods. The comparison with the contrastive, triplet and margin-based losses is important to examine the effectiveness of our original formulation, while the comparison with the other losses is to show that the formulation can be extended to the other loss functions by exploiting the proposed batch construction. Furthermore, we compare proxy-based Proxy-NCA [9] loss function with PROFS owing to its relation to our formulation. It should be noted that Proxy-NCA loss and margin-based embedding utilize GoogLeNet V2 (with batch normalization) [37] and ResNet-50 [38], respectively. Additionally, the other methods report their performances for the certain number of training iterations. To evaluate the approaches in the same basis, we retrain them by exploiting the same GoogLeNet architecture with the default hyper-parameters used in the original works except for the mini-batch and the embedding sizes as explained in the subsection 5.2 for a fair comparison.

To adapt the lifted structured loss to PROFS framework, the loss is slightly modified by ignoring the pairwise terms between the non-representative samples. For the adaptation of the sampling strategies, we trained margin-based loss with the distance weighted sampling at first. However, we were unable to acquire good results, since the distance weighted sampling is very sensitive to its parameters and we could not determine well-performing hyper-parameters. On the other hand, due to its similarity with the contrastive loss, we exploit the same hard mining strategy inspired from [11] as in the contrastive loss for the mini-batch sampling method of the margin-based loss. It should be noted that we sample one negative pair for each positive pair as in [3] for the contrastive, triplet and margin-based loss functions. Such an approach provides balance to the number of positive and negatives pairs. In the conventional hard mining, the number of hard negative pairs should match the number of positive pairs for the contrastive, triplet and margin-based loss functions. Thus, in PROFS framework, each class representative should have the same number of its corresponding positive pairs and hard negative pairs to obtain an exemplar set consistent with hard mining without violating the batch construction constraint of PROFS. Finally, no adaptation is performed for the  $N$ -pair and angular loss, since their formulation is consistent with PROFS.

### 5.4 Ablation Study

We present an ablation study to determine approximately how many training iterations,  $M$ , required to assure an acceptable approximation of the projection operation. Due to the non-convex nature of the problem, enforcing convergence for each projection might lead to ill-configured parameters that the proceeding projections cannot recover.

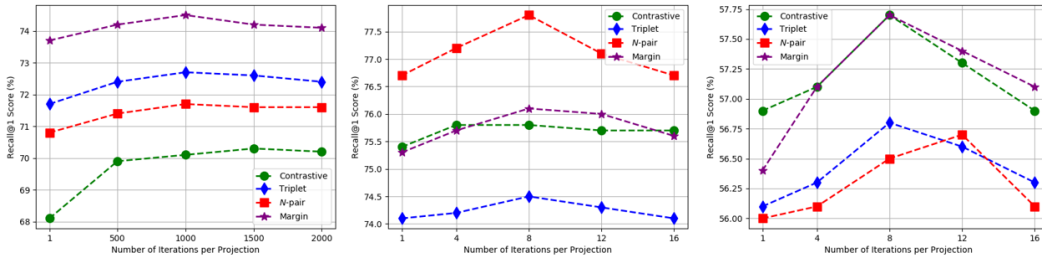


Figure 1: The retrieval performance of the PROFS on the Stanford Online Products [16] (left), the CARS196 [31] (middle) and the CUB-200-2011 [32] (right) for different number of iterations used to compute projection.

To examine effect of  $M$ , we apply PROFS framework without hard negative class mining to the contrastive, triplet,  $N$ -pair and margin loss functions on Stanford Online Products, Cars196 and CUB-200-2011. We use 2 positive images,  $I=2$ , per class in mini-batches for each loss function to have consistency among the loss terms. The retrieval performance curves for varying  $M$  values are plotted Fig. 1. The retrieval performance of each loss function improves on all three datasets as  $M$  increases up to certain values. Exceeding that certain number of iterations leads to possible over-fitting to the subproblems and the performance drops accordingly. Once the performance curves

of the different datasets are compared, an heuristic relation between  $M$  and the number of classes in a dataset can be deduced. Hence, instead of fine-tuning  $M$  parameter for each problem, we derive  $M$  as  $M = \lceil \rho/p(y_i) \rceil$  where  $\lceil \cdot \rceil$  is the ceiling function,  $p(y_i)$  denotes the probability of observing a class  $i$  in a mini-batch of size  $B$ , and  $\rho$  is how many times a class representation is to be used during the minimization. We write  $p(y_i) = B/IL$  for a batch containing  $I$  samples from each class it contains among  $L$  many classes. Considering the plots in Fig. 1, we set  $\rho=6$  throughout the experiments.

## 5.5 Quantitative Results

The quantitative results of the proposed PROFS framework with and without HNCM for the clustering and retrieval tasks on Stanford Online Products, CARS196 and CUB-200-2011 datasets are provided in Table 1 together with the baseline methods indicated in 5.3 for comparison. It can be observed that PROFS framework consistently outperforms the associated baseline methods. Compared with the original state-of-the-art loss functions, the proposed PROFS framework boosts their performance on each dataset for the clustering and retrieval tasks by up to 3.2%, 11.7% and 9.5% points on NMI,  $F_1$  and R@1 metrics, respectively. Additionally, the proposed PROFS framework with the contrastive and triplet loss functions produce competitive results in comparison with the state-of-the-art margin-based loss. It supports that considering relaxed feasible sets iteratively is beneficial over solving the entire problem at once even with the basic loss functions. This result is important to support the motivation of our formulation. Furthermore, performance improvements on the loss functions which does not directly fit in our formulation in Eq. (4.6) show that the batch construction implication of the proposed formulation can be generalized to the pairwise distance based loss functions. Apart from these, softmax-cross-entropy-like Proxy-NCA and  $N$ -pair losses yield impressive results on CARS196 and CUB-200-2011 which better fit in a classification framework owing to relatively large training data per class. However, their performance decreases dramatically compared with the other baselines on Stanford Online Products dataset which has scarce training data per class. It shows that they can not preserve the scalability of the deep metric learning methods. On the other hand, PROFS does not suffer from this degradation owing to the iterative scheme. Lastly, utilizing HNCM is more efficient on Stanford Online Products dataset, since it has almost 100 times larger number of classes than CARS196 and CUB-200-2011 datasets.

Table 1: Comparison with the state-of-the-art methods for the clustering and the retrieval tasks on Stanford Online Products [16], CARS196 [31] and CUB-200-2011 [32] datasets. Red: the overall best. Blue: the overall second best. Bold: the loss term specific best.

Method	Stanford Online Products						CARS196						CUB-200-2011					
	NMI	$F_1$	R@1	R@10	R@100	R@1000	NMI	$F_1$	R@1	R@2	R@4	R@8	NMI	$F_1$	R@1	R@2	R@4	R@8
Proxy-NCA	87.6	24.8	61.2	77.4	88.8	96.0	66.3	35.4	76.4	85.1	91.1	<b>95.1</b>	64.2	33.4	54.9	66.9	77.2	86.0
Contrastive-Hard	89.7	34.5	67.9	83.8	93.2	97.9	66.0	36.6	75.8	84.5	90.1	94.1	63.4	31.8	56.7	68.4	78.8	86.3
C-PROFS	90.3	36.4	70.1	85.4	94.1	<b>98.2</b>	<b>67.8</b>	<b>39.0</b>	76.0	84.8	90.1	<b>94.6</b>	64.1	32.0	57.7	<b>69.0</b>	78.9	86.9
C-PROFS-HNCM	<b>91.0</b>	<b>41.2</b>	<b>74.5</b>	<b>87.9</b>	<b>94.9</b>	<b>98.3</b>	66.9	38.1	<b>77.0</b>	<b>85.3</b>	<b>90.9</b>	94.4	<b>64.6</b>	<b>33.1</b>	<b>57.9</b>	<b>69.0</b>	<b>79.4</b>	<b>87.0</b>
Triplet-Semi	87.1	23.4	57.0	75.0	88.2	96.4	62.4	30.0	71.2	80.7	87.6	92.5	60.9	27.8	55.5	67.8	78.2	86.5
Triplet-Hard	88.1	30.6	65.4	81.4	91.7	97.4	62.5	30.6	71.4	81.1	87.5	92.7	63.1	30.7	56.8	68.7	78.6	86.5
T-PROFS	90.7	37.7	72.4	86.3	94.1	<b>98.1</b>	64.7	33.4	<b>74.5</b>	82.8	89.1	93.5	63.5	31.3	57.9	68.9	78.7	86.7
T-PROFS-HNCM	<b>91.3</b>	<b>42.3</b>	<b>74.9</b>	<b>87.5</b>	<b>94.4</b>	<b>98.1</b>	<b>64.9</b>	<b>33.7</b>	<b>74.5</b>	<b>83.5</b>	<b>89.4</b>	<b>93.7</b>	<b>64.5</b>	<b>32.3</b>	<b>58.1</b>	<b>69.0</b>	<b>78.9</b>	<b>86.8</b>
Lifted	88.9	31.4	66.7	83.2	91.7	97.4	60.1	27.7	67.5	77.3	84.9	90.7	60.6	26.9	53.5	65.3	75.4	84.8
L-PROFS	89.5	33.8	68.1	84.0	92.2	97.6	61.2	27.9	68.4	78.1	85.6	91.1	61.4	28.1	54.5	<b>66.1</b>	76.2	85.1
L-PROFS-HNCM	<b>89.9</b>	<b>35.1</b>	<b>69.3</b>	<b>85.1</b>	<b>93.6</b>	<b>98.1</b>	<b>61.5</b>	<b>30.0</b>	<b>70.7</b>	<b>79.6</b>	<b>86.2</b>	<b>91.5</b>	<b>62.0</b>	<b>29.5</b>	<b>54.6</b>	<b>66.1</b>	<b>76.7</b>	<b>85.5</b>
$N$ -pair	89.9	35.7	70.8	86.0	94.0	98.1	67.4	38.2	76.7	84.8	91.0	95.0	64.6	33.0	56.0	68.9	79.3	87.4
$N$ -PROFS	90.3	37.3	71.7	<b>86.6</b>	94.0	<b>98.2</b>	68.1	38.3	<b>77.8</b>	<b>85.9</b>	<b>91.6</b>	<b>95.2</b>	<b>64.9</b>	<b>33.6</b>	56.5	<b>69.0</b>	79.3	<b>87.7</b>
$N$ -PROFS-HNCM	<b>90.5</b>	<b>37.5</b>	<b>71.9</b>	<b>86.6</b>	<b>94.1</b>	<b>98.2</b>	<b>68.6</b>	<b>39.9</b>	77.6	<b>86.2</b>	<b>91.7</b>	<b>95.2</b>	<b>65.2</b>	<b>33.7</b>	<b>56.7</b>	68.8	<b>79.7</b>	87.5
Angular	90.0	36.1	72.5	86.6	93.6	97.6	66.0	35.9	77.4	85.3	91.0	94.7	61.9	29.4	54.5	66.4	76.8	84.9
A-PROFS	90.1	37.2	73.0	86.8	93.7	<b>97.7</b>	<b>66.3</b>	36.8	77.5	<b>85.6</b>	91.2	94.7	63.0	31.7	54.6	66.7	76.9	85.8
A-PROFS-HNCM	<b>90.4</b>	<b>38.4</b>	<b>73.7</b>	<b>86.9</b>	<b>93.8</b>	<b>97.7</b>	<b>66.3</b>	<b>37.9</b>	<b>77.9</b>	<b>85.6</b>	<b>91.4</b>	<b>94.8</b>	<b>64.6</b>	<b>33.4</b>	<b>55.8</b>	<b>68.1</b>	<b>78.8</b>	<b>87.3</b>
Margin-Hard	90.6	38.1	73.9	87.7	94.8	<b>98.2</b>	64.2	34.6	75.1	83.7	89.5	93.8	64.0	30.9	55.3	67.2	77.9	87.5
M-PROFS	<b>91.3</b>	<b>42.7</b>	74.5	<b>88.0</b>	<b>95.0</b>	<b>98.2</b>	64.6	35.1	76.0	84.3	89.5	93.8	64.3	<b>32.7</b>	57.7	<b>69.5</b>	<b>79.5</b>	87.5
M-PROFS-HNCM	<b>91.4</b>	<b>43.2</b>	<b>76.3</b>	<b>88.8</b>	<b>95.0</b>	<b>98.3</b>	<b>66.8</b>	<b>37.3</b>	<b>77.0</b>	<b>85.1</b>	<b>90.8</b>	<b>94.6</b>	<b>64.8</b>	32.4	<b>58.5</b>	<b>69.6</b>	<b>79.7</b>	<b>87.6</b>

## 6 Conclusion

We have presented a novel DML formulation based on alternating projections onto the feasible sets which impose relaxed proximity constraints. The resultant framework introduces a simple, yet effective, batch construction scheme. Notably, the proposed framework is applicable with the pairwise distance based state-of-the-art DML loss functions without introducing any additional computational cost. Extensive evaluations on the benchmark datasets show that the performances of the several state-of-the-art loss functions are improved by the proposed framework.

## References

- [1] Raia Hadsell, Sumit Chopra, and Yann LeCun, “Dimensionality reduction by learning an invariant mapping,” in *null*. IEEE, 2006, pp. 1735–1742.
- [2] Florian Schroff, Dmitry Kalenichenko, and James Philbin, “Facenet: A unified embedding for face recognition and clustering,” in *Proceedings of the IEEE conference on computer vision and pattern recognition*, 2015, pp. 815–823.
- [3] Chao-Yuan Wu, R Manmatha, Alexander J Smola, and Philipp Krahenbuhl, “Sampling matters in deep embedding learning,” in *Proceedings of the IEEE International Conference on Computer Vision*, 2017, pp. 2840–2848.
- [4] Jian Wang, Feng Zhou, Shilei Wen, Xiao Liu, and Yuanqing Lin, “Deep metric learning with angular loss,” in *2017 IEEE International Conference on Computer Vision (ICCV)*. IEEE, 2017, pp. 2612–2620.
- [5] Evgeniya Ustinova and Victor Lempitsky, “Learning deep embeddings with histogram loss,” in *Advances in Neural Information Processing Systems*, 2016, pp. 4170–4178.
- [6] Hyun Oh Song, Stefanie Jegelka, Vivek Rathod, and Kevin Murphy, “Deep metric learning via facility location,” in *Computer Vision and Pattern Recognition (CVPR)*, 2017, vol. 8.
- [7] Marc T Law, Raquel Urtasun, and Richard S Zemel, “Deep spectral clustering learning,” in *Proceedings of the 34th International Conference on Machine Learning-Volume 70*. JMLR. org, 2017, pp. 1985–1994.
- [8] Kihyuk Sohn, “Improved deep metric learning with multi-class n-pair loss objective,” in *Advances in Neural Information Processing Systems*, 2016, pp. 1857–1865.
- [9] Yair Movshovitz-Attias, Alexander Toshev, Thomas K Leung, Sergey Ioffe, and Saurabh Singh, “No fuss distance metric learning using proxies,” in *Proceedings of the IEEE International Conference on Computer Vision*, 2017, pp. 360–368.
- [10] Michaël Perrot and Amaury Habrard, “Regressive virtual metric learning,” in *Advances in Neural Information Processing Systems*, 2015, pp. 1810–1818.
- [11] Yuhui Yuan, Kuiyuan Yang, and Chao Zhang, “Hard-aware deeply cascaded embedding,” in *Proceedings of the IEEE international conference on computer vision*, 2017, pp. 814–823.
- [12] Ben Harwood, BG Kumar, Gustavo Carneiro, Ian Reid, Tom Drummond, et al., “Smart mining for deep metric learning,” in *Proceedings of the IEEE International Conference on Computer Vision*, 2017, pp. 2821–2829.
- [13] Weifeng Ge, “Deep metric learning with hierarchical triplet loss,” in *Proceedings of the European Conference on Computer Vision (ECCV)*, 2018, pp. 269–285.
- [14] Eric P Xing, Michael I Jordan, Stuart J Russell, and Andrew Y Ng, “Distance metric learning with application to clustering with side-information,” in *Advances in neural information processing systems*, 2003, pp. 521–528.
- [15] Kilian Q Weinberger, John Blitzer, and Lawrence K Saul, “Distance metric learning for large margin nearest neighbor classification,” in *Advances in neural information processing systems*, 2006, pp. 1473–1480.
- [16] Hyun Oh Song, Yu Xiang, Stefanie Jegelka, and Silvio Savarese, “Deep metric learning via lifted structured feature embedding,” in *Proceedings of the IEEE Conference on Computer Vision and Pattern Recognition*, 2016, pp. 4004–4012.
- [17] Marc T Law, Nicolas Thome, and Matthieu Cord, “Quadruplet-wise image similarity learning,” in *Proceedings of the IEEE International Conference on Computer Vision*, 2013, pp. 249–256.
- [18] Chen Huang, Chen Change Loy, and Xiaoou Tang, “Local similarity-aware deep feature embedding,” in *Advances in neural information processing systems*, 2016, pp. 1262–1270.
- [19] Weihua Chen, Xiaotang Chen, Jianguo Zhang, and Kaiqi Huang, “Beyond triplet loss: a deep quadruplet network for person re-identification,” in *Proceedings of the IEEE Conference on Computer Vision and Pattern Recognition*, 2017, pp. 403–412.
- [20] Yi Sun, Yuheng Chen, Xiaogang Wang, and Xiaoou Tang, “Deep learning face representation by joint identification-verification,” in *Advances in neural information processing systems*, 2014, pp. 1988–1996.
- [21] Xiaofan Zhang, Feng Zhou, Yuanqing Lin, and Shaoting Zhang, “Embedding label structures for fine-grained feature representation,” in *Proceedings of the IEEE Conference on Computer Vision and Pattern Recognition*, 2016, pp. 1114–1123.
- [22] Michael Opitz, Georg Waltner, Horst Possegger, and Horst Bischof, “Bier-boosting independent embeddings robustly,” in *Proceedings of the IEEE International Conference on Computer Vision*, 2017, pp. 5189–5198.

- [23] Wonsik Kim, Bhavya Goyal, Kunal Chawla, Jungmin Lee, and Keunjoo Kwon, “Attention-based ensemble for deep metric learning,” in *Proceedings of the European Conference on Computer Vision (ECCV)*, 2018, pp. 736–751.
- [24] Hong Xuan, Richard Souvenir, and Robert Pless, “Deep randomized ensembles for metric learning,” in *Proceedings of the European Conference on Computer Vision (ECCV)*, 2018, pp. 723–734.
- [25] Yueqi Duan, Wenzhao Zheng, Xudong Lin, Jiwen Lu, and Jie Zhou, “Deep adversarial metric learning,” in *Proceedings of the IEEE Conference on Computer Vision and Pattern Recognition*, 2018, pp. 2780–2789.
- [26] Yiru Zhao, Zhongming Jin, Guo-jun Qi, Hongtao Lu, and Xian-sheng Hua, “An adversarial approach to hard triplet generation,” in *Proceedings of the European Conference on Computer Vision (ECCV)*, 2018, pp. 501–517.
- [27] Lev M Bregman, “The relaxation method of finding the common point of convex sets and its application to the solution of problems in convex programming,” *USSR computational mathematics and mathematical physics*, vol. 7, no. 3, pp. 200–217, 1967.
- [28] Heinz H Bauschke and Adrian S Lewis, “Dykstras algorithm with bregman projections: A convergence proof,” *Optimization*, vol. 48, no. 4, pp. 409–427, 2000.
- [29] CH Pang, “Nonconvex set intersection problems: From projection methods to the newton method for super-regular sets,” *arXiv preprint arXiv:1506.08246*, 2015.
- [30] Justin Solomon, Fernando De Goes, Gabriel Peyré, Marco Cuturi, Adrian Butscher, Andy Nguyen, Tao Du, and Leonidas Guibas, “Convolutional wasserstein distances: Efficient optimal transportation on geometric domains,” *ACM Transactions on Graphics (TOG)*, vol. 34, no. 4, pp. 66, 2015.
- [31] Andreas Krause and Daniel Golovin, “Submodular function maximization.,” 2014.
- [32] Catherine Wah, Steve Branson, Peter Welinder, Pietro Perona, and Serge Belongie, “The caltech-ucsd birds-200-2011 dataset,” 2011.
- [33] Martín Abadi, Paul Barham, Jianmin Chen, Zhifeng Chen, Andy Davis, Jeffrey Dean, Matthieu Devin, Sanjay Ghemawat, Geoffrey Irving, Michael Isard, et al., “Tensorflow: a system for large-scale machine learning.,” in *OSDI*, 2016, vol. 16, pp. 265–283.
- [34] Christian Szegedy, Wei Liu, Yangqing Jia, Pierre Sermanet, Scott Reed, Dragomir Anguelov, Dumitru Erhan, Vincent Vanhoucke, and Andrew Rabinovich, “Going deeper with convolutions,” in *Proceedings of the IEEE conference on computer vision and pattern recognition*, 2015, pp. 1–9.
- [35] Olga Russakovsky, Jia Deng, Hao Su, Jonathan Krause, Sanjeev Satheesh, Sean Ma, Zhiheng Huang, Andrej Karpathy, Aditya Khosla, Michael Bernstein, et al., “Imagenet large scale visual recognition challenge,” *International journal of computer vision*, vol. 115, no. 3, pp. 211–252, 2015.
- [36] Diederik P Kingma and Jimmy Ba, “Adam: A method for stochastic optimization,” *arXiv preprint arXiv:1412.6980*, 2014.
- [37] Batch Normalization, “Accelerating deep network training by reducing internal covariate shift,” *CoRR*.–2015.–Vol. *abs/1502.03167*.–URL: <http://arxiv.org/abs/1502.03167>, 2015.
- [38] Kaiming He, Xiangyu Zhang, Shaoqing Ren, and Jian Sun, “Identity mappings in deep residual networks,” in *European conference on computer vision*. Springer, 2016, pp. 630–645.